HHS Public Access

Author manuscript

Brain Struct Funct. Author manuscript; available in PMC 2017 August 21.

Published in final edited form as:

Brain Struct Funct. 2016 April ; 221(3): 1413–1425. doi:10.1007/s00429-014-0981-8.

Deficits in task-set maintenance and execution networks in Parkinson's disease

Sule Tinaz,

Human Motor Control Section, National Institute of Neurological Disorders and Stroke, National Institutes of Health, 10 Center Drive MSC 1428, Building 10, Room 7D42, Bethesda, MD 20892, USA

Peter Lauro,

Office of the Clinical Director, National Institute of Neurological Disorders and Stroke, National Institutes of Health, Bethesda, MD 20892, USA

Mark Hallett, and

Human Motor Control Section, National Institute of Neurological Disorders and Stroke, National Institutes of Health, 10 Center Drive MSC 1428, Building 10, Room 7D42, Bethesda, MD 20892, USA

Silvina G. Horovitz

Human Motor Control Section, National Institute of Neurological Disorders and Stroke, National Institutes of Health, 10 Center Drive MSC 1428, Building 10, Room 7D42, Bethesda, MD 20892, USA

Abstract

Patients with Parkinson's disease have difficulties with self-initiating a task and maintaining a steady task performance. We hypothesized that these difficulties relate to reorganization in the sensorimotor execution, cingulo-opercular task-set maintenance, and frontoparietal adaptive control networks. We tested this hypothesis using graph theory-based network analysis of a composite network including a total of 86 nodes, derived from the three networks of interest. Resting-state functional magnetic resonance images were collected from 30 patients with Parkinson's disease (age 42–75 years, 11 females; Hoehn and Yahr score 2–3, average 2.4 ± 0.4) in their off-medication state and 30 matched control subjects (age 44–75 years, 10 females). For each node, we calculated strength as a general measure of connectivity, global efficiency and betweenness centrality as measures of functional integration, and clustering coefficient and local efficiency as measures of functional segregation. We found reduced node strength, clustering, and local efficiency in sensorimotor and posterior temporal nodes. There was also reduced node strength and betweenness centrality in the dorsal anterior insula and temporoparietal junction nodes of the cingulo-opercular network. These nodes are involved in integrating multimodal information, specifically related to self-awareness, sense of agency, and ultimately to intact

Correspondence to: Sule Tinaz.

Electronic supplementary material The online version of this article (doi:10.1007/s00429-014-0981-8) contains supplementary material, which is available to authorized users.

Conflict of interest The authors declare no conflict of interest in relation to the present manuscript.

perception of self-in-action. Moreover, we observed significant correlations between global disease severity and averaged graph metrics of the whole network. In addition to the well-known task-related frontostriatal mechanisms, we propose that the resting-state reorganization in the composite network can contribute to problems with self-initiation and task-set maintenance in Parkinson's disease.

Keywords

Resting-state; Functional magnetic resonance imaging; Graph theory; Neural network; Anterior insula; Temporoparietal junction

Introduction

Parkinson's disease (PD) is a neurodegenerative disorder characterized by motor symptoms caused by nigrostriatal dopamine depletion and cognitive symptoms related, in part, to disruption of the cognitive cortico-striatal loops (Kish et al. 1988; Grahn et al. 2008). Even during relatively early stages of the disease, patients exhibit well-known difficulties with sequential motor tasks, especially when the task is self-initiated and/or self-paced, as well as impairment in several cognitive domains including generation of internal strategies and allocation of attentional resources (Beatty and Monson 1990; Owen et al. 1993; Dubois and Pillon 1997; Zalla et al. 1998; Cools et al. 2001; Lewis et al. 2005).

Functional neuroimaging studies in PD indicated the neural substrates underlying these motor and cognitive deficits. During self-paced repetitive finger tapping or sequential finger movement tasks, patients in the off-dopamine state demonstrated a relative hypoactivation in the main task-related medial frontal regions (e.g., supplementary and pre-supplementary motor areas, and anterior cingulate cortex), and a relative hyperactivation in the lateral premotor/parietal areas and cerebellum (Samuel et al. 1997; Catalan et al. 1999; Sabatini et al., 2000; Haslinger et al. 2001; Nakamura et al. 2001; Yu et al. 2007), suggesting a functional reorganization of the sensorimotor neural substrates. Furthermore, these brain activation patterns in PD showed abnormal modulation according to the attentional demands, complexity, and context of the motor task (Catalan et al. 1999; Rowe et al. 2002).

Every task is unique with regard to its context-specific demands, and sensory inputs and motor outputs. Various components of task performance would be affected by the specific neuropathological signature of disease. However, despite their procedural differences, tasks also share basic operations: task performance begins with processing start cues and instructions. Subsequently, successful task performance depends on maintaining the mental state (task-set) across trials, while monitoring/modulating the downstream processes on a trial-by-trial basis (Dosenbach et al. 2006). A meta-analysis of task-based functional magnetic resonance imaging (fMRI) studies proposed two distinct networks to carry out these basic operations: (1) the cingulo-opercular network (CON) implements the task-set and demonstrates sustained activity across tasks. (2) The frontoparietal network (FPN) provides rapid adaptive top—down control and shows cue- and feedback-related activity (Dosenbach et al. 2006). The network properties of the CON and FPN were demonstrated

not only in task-based, but also in resting-state fMRI using graph theoretical analysis (Dosenbach et al. 2007).

Here, we propose that this general framework of top—down dual task-control mechanisms can also provide a unifying perspective for behavioral impairment in PD. Specifically, difficulties with self-initiating and/or maintaining a steady performance across self-paced tasks in PD can be conceptualized as a deficit in task-set maintenance and/or adaptive task-control. Thus, it is conceivable that the reorganization of the sensorimotor network (SMN) observed in motor task-based fMRI studies in PD would be accompanied by the reorganization of the task-set maintenance (CON) and adaptive task-control (FPN) networks.

To examine the baseline reorganization of these networks, we employed the graph theory-based network analysis on resting-state fMRI data. Of note, state-independent functional connectivity is an increasingly recognized property of neural networks. Evidence indicates that resting-state and task-specific functional connectivity patterns of a network overlap strongly (Dosenbach et al. 2007; Hoffstaedter et al. 2014), implicating that the task-free intrinsic connectivity of a network may shed light on the basic neural organization of behavior (Seeley et al. 2007). Therefore, we assumed that this approach would reveal the critical network abnormalities at rest with the advantage of avoiding the potential confounds of excessive variability in explicit behavior or effort usually associated with task-based fMRI. We created a composite network by combining the CON, FPN, and SMN nodes (Dosenbach et al. 2010) and focused our investigation on the functional segregation and integration features of this network. These features were shown to provide valuable information by demonstrating changes in network behavior in response to various types of damage in neuropsychiatric disorders (van den Heuvel et al. 2010, 2013; Rudie et al. 2012; Fair et al. 2013). We propose that deficits in functional segregation and integration in our composite network would help us to better understand the problems in self-initiating and/or maintaining a steady performance across self-paced tasks in PD.

Methods

Participants

Thirty-six PD patients (age range 42–75 years, 12 females) and 36 age- and gender-matched healthy volunteers (HV) (age range 44–75 years) participated in the study after giving written informed consent in accordance with the Combined NeuroScience Institutional Review Board of the National Institutes of Health.

All participants underwent physical and neurological examinations as well as safety screening for MRI. The following exclusion criteria applied to all participants: The presence of any neurological or psychiatric disorder (other than PD and comorbid depression or anxiety for the PD group), or a medical condition that might affect the central nervous system, abnormality in routine clinical MRI scans, active alcohol or illicit drug use, and pregnancy.

Patients were referred from the National Institutes of Health Parkinson’s Disease Clinic after a diagnosis was established according to the UK Parkinson’s Disease Society Brain Bank

Clinical Diagnosis Criteria (Hughes et al. 2001). All patients had bradykinesia and at least one of the following impairments: rigidity, resting tremor, or postural instability. Patients were assessed using the Unified Parkinson's Disease Rating Scale (UPDRS) (Fahn and Elton 1987) and the Hoehn and Yahr scale (Hoehn and Yahr 1967). All patients were scanned when they were off of any dopaminergic medication for at least 12 h (practical "off" state).

Based on our motion criteria, MRI data of six patients and six HVs were excluded. A total of 30 patients (average age = 61.2 ± 8.4, 11 females) and 30 HVs (average age = 61.4 ± 6.7, 10 females) were included in the analyses.

Image acquisition

T1-weighted anatomical images (Inversion recovery, TR: 6.536 ms, TE: 2.816 ms, TI: 450 ms, slice thickness: 1.3 mm, FoV: 240 × 240 mm, matrix size: 256 × 256) and functional MRI data (Echoplanar imaging (EPI), TR: 2 s, TE: 30 ms, flip angle: 70, FoV: 240, slice thickness: 5 mm, 3.75 × 3.75 mm in-plane resolution, axial orientation) during rest with eyes closed for 6 min and 50 s were collected with four GE Signa HDx 3T scanners with 8-channel head coils in the Nuclear Magnetic Resonance Center at the NIH. Scanning parameters were kept constant across scanners and equal numbers of HVs and patients were studied in each scanner.

Analysis

Resting-state fMRI image preprocessing—The resting-state fMRI data were analyzed using the Analysis of Functional Neuroimages (AFNI) software (Cox 1996). The afni_proc.py script for preprocessing and @ANATICOR script for noise detection and removal from resting-state time series were used. The following order of steps that was previously effective in preprocessing resting-state fMRI data was carried out (Jo et al. 2013): anatomical images of individual subjects were aligned to the first volume of EPI data via affine transformation and segmented in gray matter, white matter, and cerebrospinal fluid tissue classes. The tissue masks were subsequently resampled to EPI resolution and eroded to decrease partial volume effects. Local noise in the white matter voxel time series (i.e., noise component as a function of voxel location) was also estimated. This approach reduced the sensitivity of correlation coefficients to head motion in resting-state data. Using the local white matter mask also diminishes hardware-related noise more efficiently than the global white matter mask (Jo et al. 2010). The first two EPI volumes were removed to ensure that all remaining volumes were at magnetization steady-state. Spikes were identified in the time series. EPI volumes were slice-time corrected and motion parameters were estimated using rigid body transformations (three translations and three rotations, and their derivatives). Motion limit was 0.4 mm and outlier limit was 0.1 (i.e., 10 % of all brain voxels per TR that are above the mean absolute deviation threshold from the polynomial trend). Subsequently, anatomical images were spatially normalized to the Montreal Neurological Institute (MNI)_-caez_N27 template. The transformations involved in motion correction, co-registration, and spatial normalization steps were applied at once to the EPI data to prevent multiple resampling steps. The EPI volumes were smoothed with a 6 mm full-width half-maximum Gaussian kernel. Nuisance variables (motion, spikes, local white matter) were regressed out.

Global signal was not removed to prevent the introduction of spurious (anti)correlations (Saad et al. 2012). The time series were bandpass-filtered ($0.01 < f < 0.1$ Hz) to capture the fluctuations of the blood oxygenation level-dependent (BOLD) signal that typically occur within this frequency range at rest.

Connectivity analysis

Network definitions—A total of 86 areas of interest (nodes) were included in the network analysis. The FPN ($n = 21$), CON ($n = 32$), and SMN ($n = 33$) network nodes were derived from Dosenbach et al. (2010) (Fig. 1a, Electronic Supplementary Table 1 for all coordinates). The simple averages of the BOLD signal time courses were extracted from spheres with a radius of 5 mm centered on each node. A Pearson correlation coefficient was calculated between the average BOLD time course of each node and that of every other node. The resulting correlation adjacency matrices including all nodes were thresholded at multiple levels of the correlation coefficient "r" ($0.1 \leq r \leq 0.4$ in increments of 0.05) to ensure consistency across multiple threshold ranges. In this context, these correlation coefficients are called "connections."

We used the weighted "r" values for all graph metrics. We quantified and compared the skewness of the unthres-holded node strength distributions between the groups to ensure that the differences in graph metric results were not driven by the difference in skewness between the groups (see Electronic Supplementary Material).

Graph metric calculation—Graph metrics were calculated using custom MATLAB scripts containing functions from the Brain Connectivity Toolbox (Rubinov and Sporns 2010). For each node of the composite network, we calculated strength as a general measure of connectivity, global efficiency and betweenness centrality as measures of functional integration, and clustering coefficient and local efficiency as measures of functional segregation (see box in "Appendix: Box"). Together, these metrics allowed us to examine the functional integrity of our composite network model in the patient compared to the HV groups.

Between-group differences were assessed using permutation testing with 5000 permutations and a significance level set at $p \leq 0.05$, 2-tailed (Mattest function in Bioinformatics toolbox of Matlab 2013a). Threshold values are often arbitrarily determined and networks should ideally be characterized across a broad range of thresholds (Rubinov and Sporns 2010). For consistency, we chose stringent criteria and considered graph metrics that indicated a significant difference ($p \leq 0.05$) between the two groups at a minimum of five out of seven correlation thresholds.

Furthermore, we investigated the behavioral relevance of the graph analysis results more directly in the PD group. We calculated the nodal graph metrics averaged across the whole network per patient (i.e., one entry per patient consisting of the particular graph metric average of 86 nodes) and correlated the UPDRS total scores with the averaged whole network metrics of the PD group. We considered significant behavioral-graph metric correlations ($p \leq 0.05$) at a minimum of five out of seven thresholds.

Networks and graph metric results were graphically displayed using the Gephi (Jacomy et al. 2014) and BrainNet Viewer (Xia et al. 2013) software packages.

Post hoc seed-based whole brain functional connectivity analyses

We performed post hoc seed-based whole brain functional connectivity analyses using the nodes that showed strong and consistent differences in several graph metrics (see “Results”) as seeds. These analyses allowed us to extend our search area to the whole brain to explore the within-and between-group functional connectivity of these nodes in a broader context and to assess the potential influence of other areas outside the composite network on the functional connectivity of these nodes. To examine the relationship between the seed-based functional connectivity and behavior, we also correlated the functional connectivity of these nodes with the UPDRS total scores of the PD group.

BOLD signal time courses of the nodes were correlated with every voxel in the brain for each subject. The resulting individual functional connectivity maps were entered in one-sample *t* tests for within-group analysis and two-sample *t* tests for between-group comparisons. Within-group results were thresholded to display the top 5 % of the correlations. Between-group functional connectivity results were corrected using Monte Carlo simulations (ClustSim in AFNI). ClustSim computes the probability of a random field of noise producing a cluster of a given size after the noise is thresholded at a given level. A per-voxel *p* value threshold set at 0.001 and cluster size of 25 voxels yielded $p \leq 0.05$ corrected for the whole brain. The UPDRS total scores were used as covariates of interest separately in a simple correlation analysis with the individual functional connectivity maps. Results were corrected for the whole brain *at* $p \leq 0.05$.

Results

Participants

Average age did not differ significantly between the groups ($p = 0.9$). Details of the clinical characteristics of the patients are listed in Electronic Supplementary Material Table 2.

The onset site of motor symptoms was on the right in 19 and on the left in 11 patients. The mean Hoehn and Yahr score was 2.4 ± 0.4 (range 2–3). A Hoehn and Yahr score of 2 corresponds to mild bilateral disease without impaired balance; 2.5 to mild bilateral disease with recovery on pull test; and 3 to mild-to-moderate bilateral disease with some postural instability (Hoehn and Yahr 1967). Average disease duration was 9.5 ± 6.4 years (range 1–26 years). The UPDRS consists of four parts: Part I: mentation, behavior, and mood; Part II: activities of daily living; Part III: motor examination, and Part IV: complications of therapy. The mean total UPDRS score during the “off” period was 46.5 ± 15.2 (range 19–78) and mean “off” motor examination score was 28.4 ± 11.7 (range 6–53). None of the patients had signs of dementia as assessed using the Mini Mental State Examination test with a cut-off of 25 points (average 29.5 ± 0.8, data of two subjects are missing) (Folstein et al. 1975).

Preprocessing results

The average motion for HVs was 0.095 ± 0.04 mm and for patients 0.096 ± 0.04 mm. The average maximum displacement for HVs was 1.4 ± 0.7 mm and for patients 1.5 ± 0.8 mm. Finally, the average number of censored TRs for HVs was 4.2 ± 5.7 and for patients 6.2 ± 8.3. None of these parameters differed significantly between the groups. Final smoothing of the BOLD signal was 11 mm for both groups.

Graph metrics

The adjacency matrices showed similar correlation patterns in both groups and the average pairwise correlation strength among 86 nodes did not differ significantly between the groups ($r = 0.28$ in HV; $r = 0.25$ in patients) (Fig. 1b). The skewness of the distribution of the unthresholded node strengths was also not significantly different between the two groups (Electronic Supplementary Figs. 1, 2) indicating that skewness could not be the factor driving the graph analysis results.

Details of the between-group statistical results of the graph analysis are summarized in Table 1. Anatomical and Brodmann area labels, and MNI coordinates of these nodes are listed in Table 2.

In summary, global efficiency of the composite network did not differ between the groups. Patients showed lower node strength compared to HVs in several nodes including the left dorsal anterior insula (dAI), left temporoparietal junction (TPJ), and left posterior temporal areas in the CON, and right precentral gyrus (preCG1), right superior temporal gyrus, and right posterior insula in the SMN. The clustering coefficient was also reduced in patients mostly in the SMN nodes. Most CON and SMN nodes with lower node strength and clustering coefficient, as well as the left intraparietal sulcus in the FPN, also demonstrated reduced local efficiency in patients. In addition, the dAI and TPJ on the left (Fig. 1c) and right mid-insula nodes in the CON and right orbitofrontal gyrus node in the FPN showed lower betweenness centrality in patients.

The only metric that showed higher values in patients was the betweenness centrality in the left mid-insula and left precentral gyrus nodes in the SMN.

Correlations between graph metrics and UPDRS total scores

There was a significant positive correlation between the UPDRS total scores and the averaged nodal clustering coefficient and local efficiency of the whole network; and a significant negative correlation between the UPDRS total scores and the averaged nodal betweenness centrality of the whole network (Electronic Supplementary Table 6).

Post hoc seed-based whole brain functional connectivity

The left dAI ($x = -36$, $y = 18$, $z = 2$), left TPJ ($x = -52$, $y = -63$, $z = 15$) nodes in the CON, and right preCG1 ($x = 18$, $y = -27$, $z = 62$) node in the SMN showed strong and consistent differences in several graph metrics between the groups and were used as seeds in the whole brain functional connectivity analyses as described in “Methods”.

All three nodes demonstrated robust functional connectivity with multiple brain areas common in both groups. We reported the top 5 % of correlations of within-group functional connectivity maps for each seed (Electronic Supplementary Tables 3–5 and Electronic Supplementary Fig. 3). In both groups, the left dAI demonstrated the strongest functional connectivity with the cingulate and inferior parietal areas; the left TPJ with precuneus, ventral-lateral and superior-medial frontal, and temporal areas, and the insula; finally, the right preCG1 with the lateral premotor areas, supplementary motor area, temporal and visual areas, and insula. In addition, functional connectivity with the basal ganglia (putamen, thalamus) was also observed in the right preCG1 and left dAI in both groups.

The following differences were observed in between-group comparisons (HV > PD): the left dAI seed showed a trend of higher functional connectivity with the right angular gyrus. The left TPJ seed showed significantly stronger functional connectivity with the right orbitofrontal insula. The right preCG1 seed also demonstrated significantly stronger functional connectivity with several regions including the right precentral gyrus, left postcentral gyrus, right calcarine sulcus, bilateral superior temporal gyrus, and right supplementary motor area (Table 3, Electronic Supplementary Fig. 3). There was no brain area that showed stronger functional connectivity in the PD compared to the HV group in any of the three functional connectivity maps of interest. We did not observe significant correlations between any of the individual functional connectivity maps and the UPDRS total scores in the PD group (Electronic Supplementary Material).

Discussion

In this study, we investigated the resting-state functional integrity of top—down control and sensorimotor networks combined in mild-to-moderately affected PD patients without dementia during their off-medication state compared to their matched controls. The overall connectivity pattern and strength, as well as the global efficiency of the composite network, did not differ between the groups suggesting that this network exhibits comparable global features in both groups at rest. However, we observed reorganization of the composite network at a local (nodal) level in patients in the following ways: (1) decreased node strength indicating decreased functional connectivity which was more prominent among the CON and SMN nodes; (2) decreased clustering and local efficiency consistent with less functional segregation and less efficient local information processing primarily in the SMN nodes; and (3) decreased betweenness centrality together with reduced node strength primarily in the CON nodes implicating reduced “bridging” function and less functional integration in these nodes. Moreover, graph metrics averaged across the whole composite network correlated significantly with overall disease-related impairment. We discuss our findings in the context of functional segregation and integration of networks and relate them to behavioral manifestations unique to PD pathology.

Functional segregation

We observed reduced clustering and local efficiency in patients in several SMN and CON nodes involving the sensorimotor cortex and posterior parts of the inferior, middle, and superior temporal areas. The post hoc whole brain functional connectivity analysis using the

representative right preCG1 node as a seed corroborated these findings by revealing significantly decreased functional connectivity between the right preCG1 and other sensorimotor and temporal areas in patients.

Previous functional neuroimaging studies of motor tasks in PD did not report changes in primary sensorimotor cortical activation. Our findings of less segregated primary sensorimotor processing in a task-free state implicate that this baseline deficit might contribute to task-related functional reorganization in other sensorimotor areas in PD as summarized in the Introduction (i.e., hypoactivation inside and hyperactivation outside task-related networks).

The sensorimotor findings indicating less efficient local processing are also consistent with observations in electrophysiological studies demonstrating that the motor cortical drive in PD is slow and leads to inadequate recruitment of motor units (Brown 2000; Salenius et al. 2002). As a consequence, movements in PD are not given the full motor command that they require (Berardelli et al. 2001; Hallett 2003).

Posterior parts of the temporal areas also demonstrated less segregation in PD. These are downstream nodes involved in visuomotor processing during task-set maintenance (Dosenbach et al. 2007). A large variety of tasks based on visual perception of movement recruit these regions (Giese and Poggio 2003; Schultz et al. 2004; Pyles et al. 2007; Jastorff et al. 2011). Less segregation in these areas at rest suggests impaired visuomotor information processing at baseline that might contribute to difficulties with task-set maintenance. This finding is consistent with visuomotor processing problems in PD causing difficulties with judging distances and motion, and navigating around obstacles in everyday environments (Davidsdottir et al. 2005), as well as freezing of gait (Fahn 1995; Cowie et al. 2012; Nantel et al. 2012). Further evidence for abnormal visuomotor processing comes from a task-based fMRI study. During an optic flow task causing a perceived forward self-motion, PD patients showed less activation in the dorsal visual areas, specifically the motion perception area V5 (MT) compared to controls. However, the functional connectivity between the V5 and pre-SMA was enhanced in the PD group suggesting unbalanced motor responses due to suboptimal visuomotor processing (van der Hoorn et al. 2014).

Functional integration

The most consistent and robust findings related to functional integration among all nodes were decreased node strength and betweenness centrality in the left dAI and left TPJ nodes of the CON in patients. Basic criteria for network hub identification generally include both high connectivity and centrality (Sporns et al. 2007). In addition, the most consistent anatomical feature of hub regions is that they are multimodal association areas (Sporns et al. 2007). Both TPJ and dAI are multimodal association areas that are also anatomically connected to each other (Kucyi et al. 2012) and show stronger and more diverse connectivity with the rest of the composite network in controls. Therefore, we propose that these two areas are critical nodes in our composite network and might function as hubs, disruption of which might contribute to PD pathology in various ways.

The insula has been identified as an anatomical hub (Iturria-Medina et al. 2008). Functionally, the dAI plays a highly integrative role in many tasks (Chang et al. 2013). In a meta-analysis of functional neuroimaging studies, the dAI was found to be the overlap region for tasks assessing cognition, interoception, empathy, emotion, pain, olfaction, and gustation (Kurth et al. 2010). This overlap suggests that the dAI plays a pivotal role in integrating sensory information processed in the posterior parts and emotional valuation processed in the ventral anterior parts of the insula with cognitive appraisal. This integration is thought to give rise to the sentient self and self-awareness (Craig 2009) and set the stage for self-initiated action. Indeed, a meta-analysis of functional neuroimaging studies using self- and external agency paradigms with visual feedback demonstrated increased dAI activity during perception of self-agency (Sperduti et al. 2011). It is conceivable that integration of matching multimodal inputs (e.g., action, proprioception, visual feedback) at the dAI results in increased self-awareness and facilitates discrimination between the self and other. With respect to its role in our composite network, we think that the dAI might have the critical function of enhancing self-awareness which would be at the core of any task performance, and without which, task-set maintenance would be impossible. Thus, reduced functional connectivity and integration in the dAI observed in our PD group could be one of the basic mechanisms underlying their difficulties with self-initiating a voluntary movement and sustaining a steady performance throughout self-paced tasks.

There is also evidence linking AI dysfunction to PD pathology. Alpha-synuclein-immunoreactive inclusions, the hallmark of PD pathology, are densely deposited throughout the insula starting in stage 5 of Braak's classification (Braak et al. 2006). The AI also exhibited significant loss of dopamine D2 receptor binding in non-demented PD patients with minimal cognitive impairment. This loss correlated positively with dopaminergic depletion in the associative striatum and with the degree of executive dysfunction strengthening the view of the AI as a higher cognitive hub (Christopher et al. 2014).

The other critical node, TPJ, is also a multisensory integration area and recruited in myriad tasks ranging from basic perception to social cognition. It plays an integral role in conscious experience of the normal self and agency (Vogeley and Fink 2003; Blanke et al. 2005; Sperduti et al. 2011). A unified role for the TPJ can be conceptualized as that of a comparator of internal predictions (self, actions) with external context (space, sensory feedback) and a mismatch detector (Nahab et al. 2011). For instance, abnormal activation of the TPJ during own-body imagery affects the mental own-body transformations causing one's visual perspective and experience of self to diverge (Blanke et al. 2005). Conversely, disrupting TPJ activity enhances motor imitative ability suggesting that the motor representations of self and others converge, i.e., the other person's action cannot be inhibited and/or the self-generated motor representation cannot be activated against it, resulting in decreased control over imitation (Tsakiris et al. 2008; Sowden and Catmur 2013). This imitative facilitation is also observed in PD patients. The voluntary self-initiation problems, for instance, difficulty initiating gait after freezing, can be overcome when another person or a cue drives the action (Iansek et al. 2006). Similarly, PD patients can reverse their difficulties in task-set maintenance (e.g., progressive decline in movement speed and/or amplitude across trials during continuous tasks) when there is visual feedback or another person whose behavior they can imitate.

We think that the compromised TPJ function at rest might lead to failure to reconcile internal predictions with external context required for initiation and task-set maintenance. This failure together with reduced functional connectivity between the left TPJ and right orbitofrontal insula observed in the seed-based whole brain functional connectivity analysis in patients might, in part, be the neural basis of imitative facilitation.

Previous task-based neuroimaging studies demonstrated abnormal activation patterns in frontostriatal areas in PD patients (Owen et al. 1998; Dagher et al. 2001; Cools et al. 2002; Monchi et al. 2004; Tinaz et al. 2008, Wu et al. 2011a). Our graph and seed-based analyses revealed functional connectivity differences in a few frontal nodes between the groups. Since frontal nodes are primarily involved in adaptive top—down control, it is conceivable that dysfunction in these nodes would be more prominent during task performance rather than at rest. More recent seed-based resting-state fMRI studies also showed abnormal striatal functional connectivity and striatal—cortical remapping in PD (Helmich et al. 2010; Wu et al. 2011b; Hacker et al. 2012; Luo et al. 2014). We did not find between-group differences in striatal nodes included in the CON in graph or seed-based analyses. However, it is possible that the striatal nodes, while preserving their own functional connectivity at baseline within our selected composite network in PD, indirectly influence the functional connectivity of the other nodes in this network (Electronic Supplementary Material).

Correlations with behavior

The large-scale composite network examined here encompasses brain areas concerned with multiple behavioral domains extending beyond motor function. Similarly, in addition to the objective motor deficits, the UPDRS also evaluates patients' perceived impairment and slowness in activities of daily life such as handwriting, dressing, and gait, as well as difficulties in cognition, mood, and motivation. Therefore, the total UPDRS score provides a holistic assessment of disease-related behavioral impairment. The negative correlation between the total UPDRS scores and average nodal betweenness centrality suggests that reduced functional integration capacity across the composite network nodes might predict disease-specific behavioral impairment in PD. The unique contributions of the most affected left dAI and left TPJ nodes to this impairment need to be investigated in specific task-based studies.

We also observed positive correlations between the total UPDRS scores and average nodal clustering coefficient and local efficiency. Taken at face value, these results indicate that stronger functional segregation predicts worse behavioral impairment. However, many nodes of the composite network, primarily those belonging to the SMN, demonstrated reduced functional segregation in PD. Therefore, a neurobiologically more plausible interpretation would be reorganization in the local community structure of the composite network that might be related to behavioral impairment in PD. This resting-state local reorganization might also form the basis of task-related reorganization of the networks in PD (i.e., hypoactivation inside and hyper-activation outside task networks).

In conclusion, our results demonstrate nodal deficits in the resting-state functional integration and segregation properties of the composite network consisting of the top—down task-control and sensorimotor networks are impaired in PD. Specifically, these deficits

consist of reduced local efficiency in sensorimotor and posterior temporal areas concerned with visuomotor information processing and compromised bridging function in the TPJ and dAI, both of which are involved in integrating multimodal information. We think that this integration is crucial for self-awareness, sense of agency, and ultimately for intact perception of self-in-action. In addition to the well-known task-related frontostriatal mechanisms, we propose that these resting-state deficits constitute neural mechanisms contributing to problems with self-initiation and task-set maintenance especially in self-paced tasks in PD. Our findings reflect the changes in the task-free intrinsic connectivity of the composite network and generate multiple hypotheses for future task-based fMRI studies to probe the specific role of these compromised network nodes in actual behavioral deficits.

Supplementary Material

Refer to Web version on PubMed Central for supplementary material.

Acknowledgments

This work was supported by the National Institute of Neurological Disorders and Stroke Intramural Research Program. The authors thank Kazumi Iseki and Cecile Gallea for their help with data collection, Pritha Ghosh and Sarah Kranick for their help with patient assessments, Patrick Malone for his help with pilot data analysis, Ziad Saad for his help with data preprocessing, and Devera Schoenberg, M.Sc., for editorial assistance.

Appendix: Box

Graph metric definitions[1]

Functional segregation

Functional segregation of a neural network refers to its ability for specialized processing within clusters of nodes.

Functional integration

Functional integration is related to a neural network's ability to bind information efficiently from distributed regions.

Node strength

Node strength indicates how strongly one node is connected to the rest of the nodes in the network. It is computed as the sum of the weights of the connections that link a node to the rest of the nodes.

Path

Path is the shortest distance (i.e., minimum number of connections) between a node and every other node in the network. Efficiency is inversely related to path length.

[1]Bullmore and Sporns (2009); Rubinov and Sporns (2010).

Global efficiency

Global efficiency is calculated as the inverse of the average shortest path length between all pairs of nodes in the network. It is a measure of functional integration.

Node Betweenness

Node Betweenness Centrality indicates how central a node is to the communication among other nodes in the network. It is computed as the fraction of all shortest paths in the network that contain a given node. Nodes with high values of betweenness centrality participate in a large number of shortest paths and potentially function as hubs.

Clustering coefficient

Clustering coefficient measures the density of connections between neighboring nodes. It is computed as the number of connections that exist between the nearest neighbors of a node as a proportion of the maximum number of possible connections. High clustering is associated with high local efficiency of information transfer.

Local efficiency

Local efficiency reflects how relevant a node is for the communication among neighbors. It is computed as the inverse of the average shortest path connecting all neighbors of a node. It is a nodal measure of the average efficiency within a local neighborhood, and is related to the clustering coefficient.

References

Beatty WW, Monson N. Problem solving in Parkinson's disease: comparison of performance on the Wisconsin and California Card Sorting Tests. J Geriatr Psychiatry Neurol. 1990; 3(3):163–171. [PubMed: 2282133]

Berardelli A, Rothwell JC, Thompson PD, Hallett M. Pathophysiology of bradykinesia in Parkinson's disease. Brain. 2001; 2124(Pt 11):2131–2146.

Blanke O, Mohr C, Michel CM, Pascual-Leone A, Brugger P, Seeck M, Landis T, Thut G. Linking out-of-body experience and self processing to mental own-body imagery at the temporoparietal junction. J Neurosci. 2005; 25(3):550–557. [PubMed: 15659590]

Braak H, Bohl JR, Müller CM, Rüb U, de Vos RA, Del Tredici K. Stanley Fahn Lecture 2005: the staging procedure for the inclusion body pathology associated with sporadic Parkinson's disease reconsidered. Mov Disord. 2006; 221(12):2042–2051.

Brown P. Cortical drives to human muscle: the piper and related rhythms. Prog Neurobiol. 2000; 60(1): 97–108. [PubMed: 10622378]

Bullmore E, Sporns O. Complex brain networks: graph theoretical analysis of structural and functional systems. Nat Rev Neurosci. 2009; 10(3):186–198. DOI: 10.1038/nrn2575 [PubMed: 19190637]

Catalan MJ, Ishii K, Honda M, Samii A, Hallett M. A PET study of sequential finger movements of varying length in patients with Parkinson's disease. Brain. 1999; 122(Pt 3):483–495. [PubMed: 10094257]

Chang LJ, Yarkoni T, Khaw MW, Sanfey AG. Decoding the role of the insula in human cognition: functional parcellation and large-scale reverse inference. Cereb Cortex. 2013; 23(3):739–749. DOI: 10.1093/cercor/bhs065 [PubMed: 22437053]

Christopher L, Marras C, Duff-Canning S, Koshimori Y, Chen R, Boileau I, Segura B, Monchi O, Lang AE, Rusjan P, Houle S, Strafella AP. Combined insular and striatal dopamine dysfunction are associated with executive deficits in Parkinson's disease with mild cognitive impairment. Brain. 2014; 137(Pt 2):565–575. DOI: 10.1093/brain/awt337 [PubMed: 24334314]

Cools R, Barker RA, Sahakian BJ, Robbins TW. Mechanisms of cognitive set flexibility in Parkinson's disease. Brain. 2001; 124(Pt 12):2503–2512. [PubMed: 11701603]

Cools R, Stefanova E, Barker RA, Robbins TW, Owen AM. Dopaminergic modulation of high-level cognition in Parkinson's disease: the role of the prefrontal cortex revealed by PET. Brain. 2002; 125(Pt 3):584–594. [PubMed: 11872615]

Cowie D, Limousin P, Peters A, Hariz M, Day BL. Doorway-provoked freezing of gait in Parkinson's disease. Mov Disord. 2012; 27(4):492–499. DOI: 10.1002/mds.23990 [PubMed: 21997389]

Cox RW. AFNI: software for analysis and visualization of functional magnetic resonance neuroimages. Comput Biomed Res. 1996; 29(3):162–173. [PubMed: 8812068]

Craig AD. How do you feel—now? The anterior insula and human awareness. Nat Rev Neurosci. 2009; 10(1):59–70. DOI: 10.1038/nrn2555 [PubMed: 19096369]

Dagher A, Owen AM, Boecker H, Brooks DJ. The role of the striatum and hippocampus in planning: a PET activation study in Parkinson's disease. Brain. 2001; 124(Pt 5):1020–1032. [PubMed: 11335704]

Davidsdottir S, Cronin-Golomb A, Lee A. Visual and spatial symptoms in Parkinson's disease. Vision Res. 2005; 45(10):1285–1296. [PubMed: 15733961]

Dosenbach NU, Visscher KM, Palmer ED, Miezin FM, Wenger KK, Kang HC, Burgund ED, Grimes AL, Schlaggar BL, Petersen SE. A core system for the implementation of task sets. Neuron. 2006; 50(5):799–812. [PubMed: 16731517]

Dosenbach NU, Fair DA, Miezin FM, Cohen AL, Wenger KK, Dosenbach RA, Fox MD, Snyder AZ, Vincent JL, Raichle ME, Schlaggar BL, Petersen SE. Distinct brain networks for adaptive and stable task control in humans. Proc Natl Acad Sci USA. 2007; 104(26):11073–11078. [PubMed: 17576922]

Dosenbach NU, Nardos B, Cohen AL, Fair DA, Power JD, Church JA, Nelson SM, Wig GS, Vogel AC, Lessov-Schlaggar CN, Barnes KA, Dubis JW, Feczko E, Coalson RS, Pruett JR Jr, Barch DM, Petersen SE, Schlaggar BL. Prediction of individual brain maturity using fMRI. Science. 2010; 329(5997):1358–1361. DOI: 10.1126/science.1194144 [PubMed: 20829489]

Dubois B, Pillon B. Cognitive deficits in Parkinson's disease. J Neurol. 1997; 244(1):2–8. [PubMed: 9007738]

Fahn S. The freezing phenomenon in parkinsonism. Adv Neurol. 1995; 67:53–63. [PubMed: 8848982]

Fahn, S., Elton, R. Unified Parkinson's disease rating scale. In: Fahn, S.Marsden, CD.Calne, D., Goldstein, M., editors. Recent developments in Parkinson's disease. MacMillan Health Care Information; New Jersey: 1987. p. 153-163.

Fair DA, Nigg JT, Iyer S, Bathula D, Mills KL, Dosenbach NU, Schlaggar BL, Mennes M, Gutman D, Bangaru S, Buitelaar JK, Dickstein DP, Di Martino A, Kennedy DN, Kelly C, Luna B, Schweitzer JB, Velanova K, Wang YF, Mostofsky S, Castellanos FX, Milham MP. Distinct neural signatures detected for ADHD subtypes after controlling for micro-movements in resting state functional connectivity MRI data. Front Syst Neurosci. 2013; 6:80.doi: 10.3389/fnsys.2012.00080 [PubMed: 23382713]

Folstein MF, Folstein SE, McHugh PR. "Mini-mental state". A practical method for grading the cognitive state of patients for the clinician. J Psychiatr Res. 1975; 12(3):189–198. [PubMed: 1202204]

Giese MA, Poggio T. Neural mechanisms for the recognition of biological movements. Nat Rev Neurosci. 2003; 4(3):179–192. [PubMed: 12612631]

Grahn JA, Parkinson JA, Owen AM. The cognitive functions of the caudate nucleus. Prog Neurobiol. 2008; 86(3):141–155. DOI: 10.1016/j.pneurobio.2008.09.004 [PubMed: 18824075]

Hacker CD, Perlmutter JS, Criswell SR, Ances BM, Snyder AZ. Resting state functional connectivity of the striatum in Parkinson's disease. Brain. 2012; 135(Pt 12):3699–3711. DOI: 10.1093/brain/aws281 [PubMed: 23195207]

Hallett M. Parkinson revisited: pathophysiology of motor signs. Adv Neurol. 2003; 91:19–28. [PubMed: 12442661]

Haslinger B, Erhard P, Kämpfe N, Boecker H, Rummeny E, Schwaiger M, Conrad B, Ceballos-Baumann AO. Event-related functional magnetic resonance imaging in Parkinson's disease before and after levodopa. Brain. 2001; 124(Pt 3):558–570. [PubMed: 11222456]

Helmich RC, Derikx LC, Bakker M, Scheeringa R, Bloem BR, Toni I. Spatial remapping of cortico-striatal connectivity in Parkinson's disease. Cereb Cortex. 2010; 20(5):1175–1186. DOI: 10.1093/cercor/bhp178 [PubMed: 19710357]

Hoehn MM, Yahr MD. Parkinsonism: onset, progression and mortality. Neurology. 1967; 17(5):427–442. [PubMed: 6067254]

Hoffstaedter F, Grefkes C, Caspers S, Roski C, Palomero-Gallagher N, Laird AR, Fox PT, Eickhoff SB. The role of anterior midcingulate cortex in cognitive motor control: evidence from functional connectivity analyses. Hum Brain Mapp. 2014; 35(6):2741–2753. DOI: 10.1002/hbm.22363 [PubMed: 24115159]

Hughes AJ, Ben-Shlomo Y, Daniel SE, Lees AJ. What features improve the accuracy of clinical diagnosis in Parkinson's disease: a clinicopathologic study. Neurology. 2001; 57(10 Suppl 3):S34–S38. 1992. [PubMed: 11775598]

Iansek R, Huxham F, McGinley J. The sequence effect and gait festination in Parkinson disease: contributors to freezing of gait? Mov Disord. 2006; 21(9):1419–1424. [PubMed: 16773644]

Iturria-Medina Y, Sotero RC, Canales-Rodríguez EJ, Alemán-Gómez Y, Melie-García L. Studying the human brain anatomical network via diffusion-weighted MRI and Graph Theory. Neuroimage. 2008; 40(3):1064–1076. DOI: 10.1016/j.neuroimage.2007.10.060 [PubMed: 18272400]

Jacomy M, Venturini T, Heymann S, Bastian M. ForceAtlas2, a continuous graph layout algorithm for handy network visualization designed for the Gephi software. PLoS One. 2014; 9(6):e98679.doi: 10.1371/journal.pone.0098679 [PubMed: 24914678]

Jastorff J, Clavagnier S, Gergely G, Orban GA. Neural mechanisms of understanding rational actions: middle temporal gyrus activation by contextual violation. Cereb Cortex. 2011; 21(2):318–329. DOI: 10.1093/cercor/bhq098 [PubMed: 20513657]

Jo HJ, Saad ZS, Simmons WK, Milbury LA, Cox RW. Mapping sources of correlation in resting state FMRI, with artifact detection and removal. Neuroimage. 2010; 52(2):571–582. DOI: 10.1016/j.neuroimage.2010.04.246 [PubMed: 20420926]

Jo HJ, Gotts SJ, Reynolds RC, Bandettini PA, Martin A, Cox RW, Saad ZS. Effective preprocessing procedures virtually eliminate distance-dependent motion artifacts in resting state FMRI. J Appl Math. 2013; doi: 10.1155/2013/935154

Kish SJ, Shannak K, Hornykiewicz O. Uneven pattern of dopamine loss in the striatum of patients with idiopathic Parkinson's disease. Pathophysiologic and clinical implications. N Engl J Med. 1988; 318(14):876–880. [PubMed: 3352672]

Kucyi A, Moayedi M, Weissman-Fogel I, Hodaie M, Davis KD. Hemispheric asymmetry in white matter connectivity of the temporoparietal junction with the insula and prefrontal cortex. PLoS One. 2012; 7(4):e35589.doi: 10.1371/journal.pone.0035589 [PubMed: 22536413]

Kurth F, Zilles K, Fox PT, Laird AR, Eickhoff SB. A link between the systems: functional differentiation and integration within the human insula revealed by meta-analysis. Brain Struct Funct. 2010; 214(5–6):519–534. DOI: 10.1007/s00429-010-0255-z [PubMed: 20512376]

Lewis SJ, Slabosz A, Robbins TW, Barker RA, Owen AM. Dopaminergic basis for deficits in working memory but not attentional set-shifting in Parkinson's disease. Neuropsychologia. 2005; 43(6):823–832. [PubMed: 15716155]

Luo C, Song W, Chen Q, Zheng Z, Chen K, Cao B, Yang J, Li J, Huang X, Gong Q, Shang HF. Reduced functional connectivity in early-stage drug-naive Parkinson's disease: a resting-state fMRI study. Neurobiol Aging. 2014; 35(2):431–441. DOI: 10.1016/j.neurobiolaging.2013.08.018 [PubMed: 24074808]

Monchi O, Petrides M, Doyon J, Postuma RB, Worsley K, Dagher A. Neural bases of set-shifting deficits in Parkinson's disease. J Neurosci. 2004; 24(3):702–710. [PubMed: 14736856]

Nahab FB, Kundu P, Gallea C, Kakareka J, Pursley R, Pohida T, Miletta N, Friedman J, Hallett M. The neural processes underlying self-agency. Cereb Cortex. 2011; 21(1):48–55. DOI: 10.1093/cercor/bhq059 [PubMed: 20378581]

Nakamura T, Ghilardi MF, Mentis M, Dhawan V, Fukuda M, Hacking A, Moeller JR, Ghez C, Eidelberg D. Functional networks in motor sequence learning: abnormal topographies in Parkinson's disease. Hum Brain Mapp. 2001; 12(1):42–60. [PubMed: 11198104]

Nantel J, McDonald JC, Tan S, Bronte-Stewart H. Deficits in visuospatial processing contribute to quantitative measures of freezing of gait in Parkinson's disease. Neuroscience. 2012; 221:151–156. DOI: 10.1016/j.neuroscience.2012.07.007 [PubMed: 22796080]

Owen AM, Roberts AC, Hodges JR, Summers BA, Polkey CE, Robbins TW. Contrasting mechanisms of impaired attentional set-shifting in patients with frontal lobe damage or Parkinson's disease. Brain. 1993; 116(Pt 5):1159–1175. [PubMed: 8221053]

Owen AM, Doyon J, Dagher A, Sadikot A, Evans AC. Abnormal basal ganglia outflow in Parkinson's disease identified with PET. Implications for higher cortical functions. Brain. 1998; 121(Pt 5):949–965. [PubMed: 9619196]

Pyles JA, Garcia JO, Hoffman DD, Grossman ED. Visual perception and neural correlates of novel 'biological motion'. Vision Res. 2007; 47(21):2786–2797. [PubMed: 17825349]

Rowe J, Stephan KE, Friston K, Frackowiak R, Lees A, Passingham R. Attention to action in Parkinson's disease: impaired effective connectivity among frontal cortical regions. Brain. 2002; 125(Pt 2):276–289. [PubMed: 11844728]

Rubinov M, Sporns O. Complex network measures of brain connectivity: uses and interpretations. Neuroimage. 2010; 52(3):1059–1069. DOI: 10.1016/j.neuroimage.2009.10.003 [PubMed: 19819337]

Rudie JD, Brown JA, Beck-Pancer D, Hernandez LM, Dennis EL, Thompson PM, Bookheimer SY, Dapretto M. Altered functional and structural brain network organization in autism. Neuroimage Clin. 2012; 2:79–94. DOI: 10.1016/j.nicl.2012.11.006 [PubMed: 24179761]

Saad ZS, Gotts SJ, Murphy K, Chen G, Jo HJ, Martin A, Cox RW. Trouble at rest: how correlation patterns and group differences become distorted after global signal regression. Brain Connect. 2012; 2(1):25–32. DOI: 10.1089/brain.2012.0080 [PubMed: 22432927]

Sabatini U, Boulanouar K, Fabre N, Martin F, Carel C, Colonnese C, Bozzao L, Berry I, Montastruc JL, Chollet F, Rascol O. Cortical motor reorganization in akinetic patients with Parkinson's disease: a functional MRI study. Brain. 2000; 123(Pt 2):394–403. [PubMed: 10648446]

Salenius S, Avikainen S, Kaakkola S, Hari R, Brown P. Defective cortical drive to muscle in Parkinson's disease and its improvement with levodopa. Brain. 2002; 125(Pt 3):491–500. [PubMed: 11872607]

Samuel M, Ceballos-Baumann AO, Blin J, Uema T, Boecker H, Passingham RE, Brooks DJ. Evidence for lateral premotor and parietal overactivity in Parkinson's disease during sequential and bimanual movements. A PET study. Brain. 1997; 120(Pt 6):963–976. [PubMed: 9217681]

Schultz J, Imamizu H, Kawato M, Frith CD. Activation of the human superior temporal gyrus during observation of goal attribution by intentional objects. J Cogn Neurosci. 2004; 16(10):1695–1705. [PubMed: 15701222]

Seeley WW, Menon V, Schatzberg AF, Keller J, Glover GH, Kenna H, Reiss AL, Greicius MD. Dissociable intrinsic connectivity networks for salience processing and executive control. J Neurosci. 2007; 27(9):2349–2356. [PubMed: 17329432]

Sowden S, Catmur C. The role of the right temporoparietal junction in the control of imitation. Cereb Cortex. 2013 (Epub ahead of print).

Sperduti M, Delaveau P, Fossati P, Nadel J. Different brain structures related to self- and external-agency attribution: a brief review and meta-analysis. Brain Struct Funct. 2011; 216(2):151–157. DOI: 10.1007/s00429-010-0298-1 [PubMed: 21212978]

Sporns O, Honey CJ, Kötter R. Identification and classification of hubs in brain networks. PLoS One. 2007; 2(10):e1049. [PubMed: 17940613]

Tinaz S, Schendan HE, Stern CE. Fronto-striatal deficit in Parkinson's disease during semantic event sequencing. Neurobiol Aging. 2008; 29(3):397–407. [PubMed: 17157417]

Tsakiris M, Costantini M, Haggard P. The role of the right temporo-parietal junction in maintaining a coherent sense of one's body. Neuropsychologia. 2008; 46(12):3014–3018. DOI: 10.1016/j.neuropsychologia.2008.06.004 [PubMed: 18601939]

van den Heuvel MP, Mandl RC, Stam CJ, Kahn RS, Hulshoff Pol HE. Aberrant frontal and temporal complex network structure in schizophrenia: a graph theoretical analysis. J Neurosci. 2010; 30(47):15915–15926. DOI: 10.1523/JNEUROSCI.2874-10.2010 [PubMed: 21106830]

van den Heuvel MP, Sporns O, Collin G, Scheewe T, Mandl RC, Cahn W, Goñi J, Hulshoff Pol HE, Kahn RS. Abnormal rich club organization and functional brain dynamics in schizophrenia. JAMA Psychiatry. 2013; 70(8):783–792. DOI: 10.1001/jamapsychiatry.2013.1328 [PubMed: 23739835]

van der Hoorn A, Renken RJ, Leenders KL, de Jong BM. Parkinson-related changes of activation in visuomotor brain regions during perceived forward self-motion. PLoS One. 2014; 9(4):e95861.doi: 10.1371/journal.pone.0095861 [PubMed: 24755754]

Vogeley K, Fink GR. Neural correlates of the first-person-perspective. Trends Cogn Sci. 2003; 7(1): 38–42. [PubMed: 12517357]

Wu T, Wang L, Hallett M, Chen Y, Li K, Chan P. Effective connectivity of brain networks during self-initiated movement in Parkinson's disease. Neuroimage. 2011a; 55(1):204–215. DOI: 10.1016/j.neuroimage.2010.11.074 [PubMed: 21126588]

Wu T, Long X, Wang L, Hallett M, Zang Y, Li K, Chan P. Functional connectivity of cortical motor areas in the resting state in Parkinson's disease. Hum Brain Mapp. 2011b; 32(9):1443–1457. DOI: 10.1002/hbm.21118 [PubMed: 20740649]

Xia M, Wang J, He Y. BrainNet Viewer: a network visualization tool for human brain connectomics. PLoS One. 2013; 8:e68910. [PubMed: 23861951]

Yu H, Sternad D, Corcos DM, Vaillancourt DE. Role of hyperactive cerebellum and motor cortex in Parkinson's disease. Neuroimage. 2007; 35(1):222–233. [PubMed: 17223579]

Zalla T, Sirigu A, Pillon B, Dubois B, Grafman J, Agid Y. Deficit in evaluating pre-determined sequences of script events in patients with Parkinson's disease. Cortex. 1998; 34(4):621–627. [PubMed: 9800095]

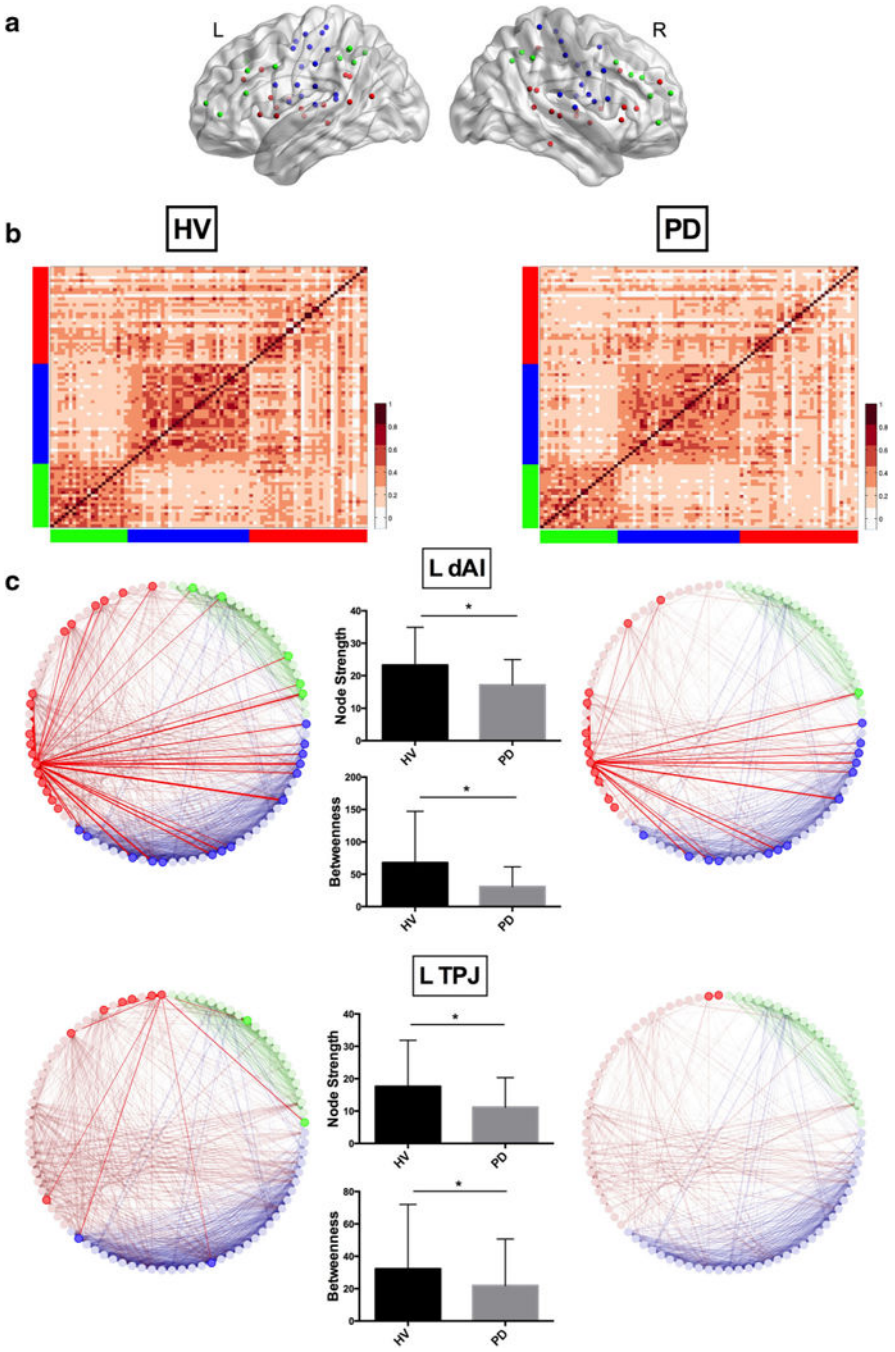

Fig. 1.

a Locations of the composite network nodes are shown on left and right hemispheres (*red* CON, *green* FPN, *blue* SMN). b Heatmaps of the adjacency matrices demonstrate the raw pairwise correlations between composite network nodes ($r = 0.28$ in HV; $r = 0.25$ in PD). *Red* CON, *green* FPN, *blue* SMN, *HV* Healthy volunteer group, *PD* Parkinson's disease group. c Connectivity patterns of the left dorsal anterior insula (dAI) and left temporoparietal junction (TPJ) are displayed at a threshold of $r = 0.35$. This threshold was chosen arbitrarily for display purposes. The *bar graphs* show the mean (±SD) node strength

and betweenness centrality for each node in both groups. HV *(left column)*: left dAI showed connections with FPN nodes in the anterior prefrontal cortex, anterior cingulate cortex, and inferior parietal lobe; with CON nodes in the anterior cingulate cortex, mid-cingulate gyrus, ventral prefrontal cortex, mid-insula and posterior insula, superior temporal gyrus, middle temporal gyrus, inferior parietal lobe, and precuneus; and with SMN nodes in the supplementary and pre-supplementary motor areas, precentral gyrus, mid-insula and posterior insula, and superior temporal gyrus. Left TPJ showed connections with FPN nodes in the ventral prefrontal cortex and inferior parietal lobe; with CON nodes in the ventral prefrontal cortex, superior temporal gyrus, and inferior parietal lobe; and with SMN nodes in the superior temporal gyrus. *PD (right column):* left dAI showed connections with FPN nodes in the anterior cingulate cortex; with CON nodes in the anterior cingulate cortex, mid-cingulate gyrus, ventral prefrontal cortex, mid-insula, superior temporal gyrus; and SMN nodes in the supplementary and pre-supplementary motor areas, precentral gyrus, mid-insula and posterior insula, and superior temporal gyrus. Left TPJ showed connections only with one CON node in the middle temporal gyrus

Table 1

Changes in graph metrics in PDs compared with HVs

Node strength	Clustering	Local efficiency	Betweenness
CON			
L dAI↓	R IFG pars Tri↓^	L post MTG/STG↓	L dAI↓
R ITG↓		L TPJ↓	L TPJ↓^
L post MTG/STG↓		R ITG↓*	R MI↓^
L TPJ↓		R STG↓*	
FPN			
–	–	L IPS↓^	R OFG↓^
SMN			
R preCG1↓	R preCG1↓	R preCG1↓	L MI↑
L STG1↓	L preCG1↓	L preCG1↓	L preCG2↑
RPI↓^	L preCG2↓*	R preCG3↓*	
	L STG2↓	L STG1↓^	
	R postCG↓*	L STG3↓^	
	L postCG↓^		
	R preCG2↓^		

The up and down arrows display the significant changes in graph metrics in PD relative to the HV group. Note that the node labels in this study were determined based on the MNI probabilistic maps in AFNI

CON cingulo-opercular network, *FPN* frontoparietal network, *SMN* sensorimotor network, *L* left, *R* right, post posterior, *dAI* dorsal anterior insula, *ITG* inferior temporal gyrus, *MTG* middle temporal gyrus, *STG* superior temporal gyrus, *TPJ* temporoparietal junction, *IFG* inferior frontal gyrus, *Tri* triangularis, *preCG* precentral gyrus, *postCG* postcentral gyrus, *OFG* orbitofrontal gyrus, *IPS* intraparietal sulcus, *MI* midinsula, *PI* posterior insula

*$p \leq 0.05$ at six out of seven and

^$p \leq 0.05$ at five out of seven correlation thresholds ($0.1 \leq r \leq 0.4$ in increments of 0.05). For all other nodes, $p \leq 0.05$ across seven correlation thresholds

Table 2

MNI coordinates and BA labels of significant nodes

	BA	*x*	*y*	*z*
CON				
L dAI	13	−36	18	2
R ITG	20	54	−31	−18
L post MTG/STG	21/22	−59	−47	11
L TPJ		−52	−63	15
R IFG pars Tri	45	51	23	8
R STG[a]	22	58	−41	20
R MI	13	32	−12	2
FPN				
L IPS		−32	−58	46
R OFG	10	42	48	−3
SMN				
R preCG1	4	18	−27	62
R preCG2[b]	4	41	−23	55
R preCG3	4	44	−11	38
L preCG1[b]	4	−24	−30	64
L preCG2	4	−38	−27	60
R postCG	1	34	−39	65
L postCG	3	−47	−18	50
L STG1	41	−53	−37	13
L STG2	41	−41	−37	16
L STG3	41	−54	−22	9
R PI	13	42	−24	17
L MI	13	−36	−12	15

The MNI coordinates and Brodmann area (BA) labels of nodes that showed statistically significant differences in graph metrics between the groups are listed

CON cingulo-opercular network, *FPN* frontoparietal network, *SMN* sensorimotor network, *L* left, *R* right, *post* posterior, *dAI* dorsal anterior insula, *ITG* inferior temporal gyrus, *MTG* middle temporal gyrus, *STG* superior temporal gyrus, *TPJ* temporoparietal junction, *IFG* inferior frontal gyrus, *Tri* triangularis, *preCG* precentral gyrus, *postCG* postcentral gyrus, *OFG* orbitofrontal gyrus, *IPS* intraparietal sulcus, *MI* mid-insula, *PI* posterior insula

[a] Inferior parietal lobule is within 1 mm

[b] Postcentral gyrus (BA3) is within 1 mm

Table 3

Between-group comparisons of seed-based functional connectivity results

HV > PD	BA	*x*	*y*	*z*	Z value
Left dAI					
R angular gyrus[a]	39	46	−75	38	4.16
Left TPJ					
R OFI	47/12	42	30	−11	4.23
R preCG1					
R preCG	4/6	49	−12	49	4.94
L postCG	3	−60	−5	24	4.36
R calcarine	18	21	−61	17	4.37
R STG	22	67	−23	0	4.13
L STG	22	−56	−40	14	4.01
R SMA	6	7	−19	49	4.12

$p \leq 0.05$ corrected for the whole brain. Per-voxel *p* value threshold set at 0.001 and cluster size of 25 voxels

HV healthy volunteer group, *PD* parkinson's disease group, *L* left, *R* right, *dAI* dorsal anterior insula, *TPJ* temporoparietal junction, *OFI* orbitofrontal insula, *preCG* precentral gyrus, *postCG* postcentral gyrus, *STG* superior temporal gyrus, *SMA* supplementary motor area

[a]This is a trend with a per-voxel *p* value set to 0.0016 and cluster size of 25 voxels